Synthesis of Bandpass Filter as a Four-Pole Based on a Non-Homogeneous Line

Valeriy Kozlovskiy[1], Valerii Kozlovskiy[2], Juliy Boiko[3], Yuriy Balanyuk[4], Natalia Yakymchuk[5]
[1,4]Department of Information Protection, National Aviation University, Ukraine
[2]Special Department no. 4 of the Institute of Special Communication and Information Protection, National Technical University of Ukraine "Kyiv Polytechnic Institute", Ukraine
[3]Department of Telecommunications, Media and Intelligent Technologies, Khmelnytskyi National University, Ukraine
[5]Department of Electronics and Telecommunications, Lutsk National Technical University, Ukraine

Article Info

Article history:

Received Apr 15, 2024
Revised Jun 28, 2024
Accepted Jul 18, 2024

Keywords:

Four-pole
Heterogeneous line
Impedance
Filter
Matching device

ABSTRACT

The article deals with the synthesis of band-pass filters (BPF) for the design of microwave filtering devices, by using non-homogeneous lines (NL) with the selection of the appropriate wave impedance *W*. For this purpose, equivalent NL substitution circuits were created in the region of resonant and anti-resonant frequencies, and four-pole matrices of the transmission line were determined, whose matrix of impedances and admittances does not have partial poles, and the transmission admittance and transmission impedance do not have zeros. BPF prototypes were synthesized with two parallel plumes based on a closed homogeneous line and one plume based on three NLs. A band-pass filter with an extended blocking band was implemented, and its amplitude-frequency characteristics were obtained. The use of NLs as resonators allows the choice of wave impedance to increase the blocking band of the BPF compared to the BPF on resonators based on homogeneous lines.

Corresponding Author:

Juliy Boiko,
Department of Telecommunications, Media and Intelligent Technologies,
Khmelnytskyi National University,
11, Instytuts'ka str., Khmelnytskyi, 29016, Ukraine.
Email: boiko_julius@ukr.net

1. INTRODUCTION

The development of radio communication and broadcasting systems is largely determined by the efficiency of using radio frequency resources, the possibility of expanding working frequency bands and simultaneously narrowing protective frequency bands between channels, as well as ensuring a wide range of quality parameters of modern telecommunication services [1]. Frequency selection devices (filters) are the most important component of the channel-forming and group equipment of wireless transmission systems and largely determine the characteristics of the entire radio transmission system in general. At the same time, these devices must have minimal losses in the bandwidth, the widest blocking band, and minimal weight and size indicators [2, 3]. Taking into account the fact that the technical characteristics of radio technical devices depend significantly on the parameters of the filters, the intensive development of new types of filters that work in ultra-high frequency ranges is actively continued [4, 5].

When designing various microwave devices, transmission lines with constant wave impedance (homogeneous lines HL), which have periodic amplitude-frequency characteristics, are widely used, which causes the presence of parasitic channels for receiving filters and matching devices [6]. There is clearly a need to develop more advanced filter structures suitable for integration with modern telecommunications equipment. To a large extent, you can get rid of this drawback when using NL by selecting the appropriate wave impedance, the value of which depends on the current length. To design filter-matching devices for any purpose, you need to know the matrix of the NL, considered as a four-pole. In this case, with a known NL matrix, any method of synthesizing filters or matching circuits can be used. Therefore, the main task when using NL as a filter element is to determine the four-pole matrix of the transmission line [7].

In the general case, the problem of determining any four-pole matrix does not have a closed exact solution, since the processes in NL are described by second-order differential equations, the solution of which is expressed in quadratures only in some particular cases. As a result, the definition of exact final expressions for the elements of matrices of four-poles based on the NL is possible for individual special cases, which does not allow for realizing the potential of the NL.

The analysis of recent studies shows that today several groups of methods for the synthesis of broadband filtering devices are used simultaneously.

Most often, in the synthesis of distributed filters and matching circuits, classical analytical methods are used, which involve the construction of filters based on resonators interconnected by impedance or conductivity inverters [8-10]. This method allows you to implement the frequency response with a minimum number of resonators and is suitable mainly for the construction of filters with active constant loads. Thus, a method of direct synthesis of coupled symmetrical resonator filters with source-load coupling was developed [11]. If the active load depends on the frequency, then the construction of filters will be performed only in a narrow range of frequencies (the relative bandwidth is units of percent). Also, the use of classical methods for homogeneous lines has disadvantages related to the fact that it is impossible to obtain arbitrary transmission characteristics [12], one must rely on time-consuming parametric studies to obtain the design parameters of the device.

The use of the method of characteristic parameters in the construction of distributed filters is now rarely used due to the complexity of calculating the characteristic impedances of filter elements built on the basis of uniform lines with included concentrated non-homogeneities. The study of the influence of the microwave devices' design parameters on the electrical characteristics of filter lines and matching lines should take into account the deviation of the wave impedance from the nominal values.

Match the amplitude-frequency characteristics of the filters with the load, possible when using elements of NL. This is done by selecting the appropriate impedance of the line, which improves the appearance of the amplitude-frequency characteristics and allows you to avoid the parasitic receiving channels of filters [13].

However, today a small number of NLs for which the solutions of telegraph equations are known are described, which limits the elemental basis for the construction of microwave telecommunication systems and prevents the development of devices with the necessary amplitude-frequency characteristics [13]. At present, exact solutions of telegraph equations are known for lines that are most widely used in practice, with an exponential change in wave impedance, with parabolic and hyperbolic wave impedance [14-16]. In the case of other types of lines, numerical methods are used [17], the disadvantage of which is the partial character of the obtained results.

The experience of using 3D printing to create the structure of microwave components, which are then covered with metal to build a conductive layer, provides wide opportunities for practical application of the new element base for the construction of microwave devices [18, 19]. The proposed 3D printing methods reduce the cost of components, which does not depend on the complexity of the product and are lighter compared to conventional metal ones.

The purpose of the article is to expand the element base of heterogeneous lines for the design of microwave filter-matching devices.

2. RESEARCH METHOD

In this section presents the conclusion of the determination of the NL conductivity matrix. Substitution circuit in the region of resonant frequencies is presented and described. The issues of formation and mathematical description of the substitution circuit of anti-resonant frequencies have been separately developed.

2.1. The Determination of the NL Conductivity Matrix

To determine the four-pole NL matrices, it is proposed to use the properties of the line as a four-pole with a compact residue [20], the matrix of impedances and admittances of which does not have partial poles, and the transfer conductivity and transfer impedance do not have zeros. This allows you to find all elements of the matrix of impedances and admittances by the input impedance of an open line (the input conductivity of a closed line).

Let's use this method to determine the conductivity matrix of the NL with wave impedance $W(\tau) = W_0 / ch^2 a\tau$, where τ is the current delay time, α is a positive number, W_0 is the wave impedance at the beginning of the line. In this case, the element y_{11} of the conductivity matrix Y is:

$$y_{11} = \frac{\sqrt{p^2+a^2}}{pW_0 th\sqrt{p^2+a^2}t} = \frac{\sqrt{p^2+a^2}ch\sqrt{p^2+a^2}t}{pW_0 sh\sqrt{p^2+a^2}t} \quad (1)$$

Equating the denominator to zero, we find the poles $p_k = j\omega_k$ for conduction y_{11}:

$$p_0 = 0,\ \omega_k^2 = \left(\frac{k\pi}{t}\right)^2 + a^2,\ k = 1,2,... \quad (2)$$

Following [3], we find the transfer conductivity:

$$-y_{12} = \frac{1}{pL_{st}\prod_{k=1}^{\infty}\left(1+\frac{p_k^2}{\omega_k^2}\right)}, \quad (3)$$

Where L_{st} is the static inductance of the line:

$$L_{SI} = \int_0^t W(\tau)d\tau = \int_0^t \frac{W_0}{ch^2 a\tau}d\tau = \frac{W_0}{a} that. \quad (4)$$

From here we find the transfer conductivity:

$$-y_{12} = \frac{1}{\frac{W_0 p}{chat}\frac{sh\sqrt{p^2+a^2}t}{\sqrt{p^2+a^2}}}. \quad (5)$$

Note that at the $p \to 0$ conductivity ($-y_{12}$) tends to the conductivity of the static inductance L_{st}, and at the $\alpha \to 0$ conductivity is $-y_{12} \to \frac{1}{W_0 shpt}$, that is, in the limiting case, we have the conductivity of a homogeneous line with a wave impedance W_0 and a delay time *t*.

Find the element y_{22} of the matrix of conductivities. To do this, we use the condition of compact residue of the elements of the admittance matrix of a non-homogeneous line [14].

$$k_{11}^{(m)}k_{22}^{(m)} - \left(k_{12}^{(m)}\right)^2 = 0 \quad (6)$$

Where $k_{11}^{(m)}, k_{22}^{(m)}, k_{12}^{(m)}$ are the residues of the elements y_{11}, y_{22}, y_{12}.

Residues are coefficients in the expansion of a fractional-rational function into a sum of simple fractions and for lossless circuits are determined by the expression [14].

$$k_{ij}^{(m)} = \frac{P(p_m)}{Q'(p_m)},\quad i = 1,2;\ j = 1,2;\ m = 1,2,... \quad (7)$$

Where *P* is the function numerator polynomial, *Q* is the denominator polynomial, p_m are the roots of the denominator.

By residues and poles, the elements of the matrix of conductivities (impedances) of lossless circuits are determined [21]. In particular, if the conductivities have a pole at zero, as in our case, then the elements of the admittance matrix can be represented as (for different elements y_{ij} the polynomials *P* and *Q* are different) [14]:

$$y_{ij} = \frac{P(p)}{Q(p)} = \frac{k_{ij}^{(0)}}{p} + \sum_{m=1}^{\infty}\frac{2k_{ij}^{(m)}}{P^2+\omega_m^2},\ i = 1,2;\ j = 1,2;\ k_{ij}^{(0)} = \frac{1}{L_{st}} \quad (8)$$

In view of what has been said, we find the residues y_{11}. To do this, we write y_{11} in the form:

$$y_{11} = \frac{P(p)}{Q(p)} = \frac{ch\sqrt{p^2+a^2}t}{\frac{pW_0 sh\sqrt{p^2+a^2}t}{\sqrt{p^2+a^2}}} = \frac{k_{11}^{(0)}}{p} + \sum_{m=1}^{\infty}\frac{2k_{11}^{(m)}}{P^2+\omega_m^2}. \quad (9)$$

In our case:

$$Q(p) = \frac{W_0 psh\sqrt{p^2+a^2}t}{\sqrt{p^2+a^2}},\ P(p) = ch\sqrt{p^2+a^2}t. \quad (10)$$

We find the residues for:

$$p = j\omega_m = p_m,\ \omega_m^2 = \left(\frac{m\pi}{t}\right)^2 + a^2,\ m = 1,2,... .$$

$$k_{11}^{(m)} = \frac{P(p_m)}{Q'(p_m)} = \frac{\cosh\left(\sqrt{p^2+a^2}\cdot t\right)}{W_0\left(\frac{d}{dp}\cdot\frac{p\cdot\sinh\left(\sqrt{p^2+a^2}\cdot t\right)}{\sqrt{p^2+a^2}}\right)} = \frac{(p^2+a^2)^{\frac{3}{2}}}{W_0}\times$$

$$\times\frac{\cosh\left(\sqrt{p^2+a^2}\cdot t\right)}{\left(\sinh[\sqrt{p^2+a^2}\cdot t]a^2 + p^2\cosh[\sqrt{p^2+a^2}\cdot t]\cdot t\cdot\sqrt{p^2+a^2}\right)} \quad (11)$$

Similarly, we define the residues of the element y_{12}. Given that:

$$-y_{12} = \frac{P(p)}{Q(p)} = \frac{1}{\frac{W_0 p}{chat}\frac{sh\sqrt{p^2+a^2}t}{\sqrt{p^2+a^2}}},$$

$$P(p)=1,\ Q(p) = \frac{W_0 p}{chat}\frac{sh\sqrt{p^2+a^2}t}{\sqrt{p^2+a^2}}, \quad (12)$$

find ($p=p_m$):

$$k_{12}^{(m)} = \frac{-\cosh(a\cdot t)}{W_0\left(\frac{d}{dp}\cdot\frac{p\cdot\sinh\left(\sqrt{p^2+a^2}\cdot t\right)}{\sqrt{p^2+a^2}}\right)} = \frac{\left(p^2+a^2\right)^{\frac{3}{2}}}{W_0}\times$$

$$\times\frac{-\cosh(a\cdot t)}{\left(\sinh[\sqrt{p^2+a^2}\cdot t]a^2 + p^2\cosh[\sqrt{p^2+a^2}\cdot t]\cdot t\cdot\sqrt{p^2+a^2}\right)} \quad (13)$$

Thus, the transfer conductivity and the element y_{22} of the conductivity matrix take the form:

$$y_{12} = \frac{k_{12}^{(0)}}{p} + \sum_{m=1}^{\infty}\frac{2k_{12}^{(m)}}{P^2+\omega_m^2},\ i=1,2;\ j=1,2;\ k_{12}^{(0)} = \frac{1}{L_{st}}, \quad (14)$$

$$y_{22} = \frac{k_{22}^{(0)}}{p} + \sum_{m=1}^{\infty}\frac{2k_{22}^{(m)}}{P^2+\omega_m^2},\ i=1,2;\ j=1,2;\ k_{22}^{(0)} = \frac{1}{L_{L_{st}}}. \quad (15)$$

The residues $k_{22}^{(m)}$ are found from the compactness condition (6) $k_{11}^{(m)}k_{22}^{(m)} - \left(k_{12}^{(m)}\right)^2 = 0$:

$$k_{22}^{(m)} = \frac{\left(k_{12}^{(m)}\right)^2}{k_{11}^{(m)}}. \quad (16)$$

Thus, the matrix of conductivities is completely defined. Knowing the matrix of conductivities, it is possible to synthesize various types of filters or matching devices using known methods [15, 16], [22, 23].

Consider the synthesis of bandpass filters (BPF). To do this, we first determine the equivalent circuits of the NL in the region of the poles of the elements of the matrix of impedances and conductivities.

2.2. Substitution Circuit in the Region of Resonant Frequencies

For lossless lines, the impedance matrix can be written as:

$$[Z] = [Z]_0 + \sum_{\nu=1}^{\infty}[Z]_\nu,\ [Z]_0 = \frac{1}{pC_{st}}\begin{bmatrix}1 & 1\\ 1 & 1\end{bmatrix},$$

$$[Z]_\nu = \frac{2p}{p^2+\omega_\nu^2}\left[k_{mn}^{(\nu)}\right],\ \nu=1,2, \quad (17)$$

Where C_{st} is the static capacitance of the line; $\left[k_{mn}^{(\nu)}\right]$ - matrix of residues of the elements of the matrix of impedances in the poles $p_\nu = j\omega_\nu,\ \nu=1,2,3,...,\ m=1,2;\ n=1,2$.

$$\left[k_{mn}^{(\nu)}\right] = \begin{bmatrix} resZ_{11} & resZ_{12}\\ resZ_{12} & resZ_{22}\end{bmatrix} \quad (18)$$

From (17), (18) it follows that in the region of the resonant frequency ω_ν, that is, in the region of the pole $p_\nu = j\omega_\nu$, there is an approximate equality:

$$[Z]\approx[Z]_\nu=\begin{bmatrix}\dfrac{2k_{11}^{(\nu)}p}{p^2+\omega_\nu^2} & \dfrac{2k_{12}^{(\nu)}p}{p^2+\omega_\nu^2}\\ \dfrac{2k_{12}^{(\nu)}p}{p^2+\omega_\nu^2} & \dfrac{2k_{22}^{(\nu)}p}{p^2+\omega_\nu^2}\end{bmatrix} \quad (19)$$

Since the line is a compact four-pole:

$$k_{11}^{(\nu)}k_{22}^{(\nu)}-\left(k_{12}^{(\nu)}\right)^2=0, \quad (20)$$

then matrix (19), taking into account (20), can be implemented in the form of a four-pole circuit in Figure 1.

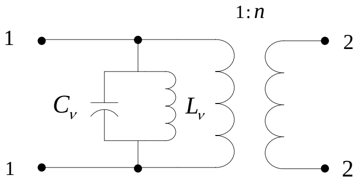

Figure 1. Equivalent circuit of a non-homogeneous line in the region of resonant frequencies

To prove it, let's find the elements of the impedance matrix of the circuit in Figure 1. Let's imagine this circuit as a cascade connection of a circuit and an ideal transformer. Then the elements of the impedance matrix of the circuit will be written in the form [20]:

$$Z_{11}=\frac{\frac{1}{C_\nu}p}{p^2+\omega_\nu^2},\ Z_{22}=\frac{\frac{n^2}{C_\nu}p}{p^2+\omega_\nu^2},\ Z_{12}=\frac{\frac{n}{C_\nu}p}{p^2+\omega_\nu^2} \quad (21)$$

Comparing (21) with (19), we find:

$$C_\nu=\frac{1}{2k_{11}^{(\nu)}},\ L_\nu=\frac{2k_{11}^{(\nu)}}{\omega_\nu^2},\ n=\frac{k_{12}^{(\nu)}}{k_{11}^{(\nu)}}=\frac{k_{22}^{(\nu)}}{k_{12}^{(\nu)}} \quad (22)$$

Similarly, one can obtain the second equivalent circuit in Figure 2.

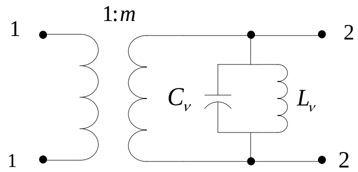

Figure 2. The second equivalent circuit of a non-homogeneous line in the resonant frequency region

In this case, the elements of the impedance matrix, as follows from Figure 2, have the form:

$$Z_{11}=\frac{1}{m^2}\frac{\frac{1}{C_\nu}p}{p^2+\omega_\nu^2},\ Z_{22}=\frac{\frac{1}{C_\nu}p}{p^2+\omega_\nu^2},\ Z_{12}=\frac{1}{m}\frac{\frac{1}{C_\nu}p}{p^2+\omega_\nu^2} \quad (23)$$

Comparing (23) with (19), we obtain:

$$C_\nu=\frac{1}{2k_{22}^{(\nu)}},\ L_\nu=\frac{2k_{22}^{(\nu)}}{\omega_\nu^2},\ m=\frac{k_{12}^{(\nu)}}{k_{11}^{(\nu)}}=\frac{k_{22}^{(\nu)}}{k_{12}^{(\nu)}} \quad (24)$$

That is, the transformation ratio for both circuits in Figure 1, Figure 2 is the same. The difference is observed in the definition of inductance and capacitance of the circuit.

2.3. Substitution Circuit of Anti-Resonant Frequencies

Under the anti-resonant frequency is understood the frequency of series resonance, that is, when the conductivity of the circuit without loss turns to infinity. In other words, the anti-resonance frequencies are determined by the input conduction poles in the plane of the complex frequency variable.

For lossless lines, the matrix of conductivities can be written as:

$$[Y]=[Y]_0+\sum_{\nu=1}^{\infty}[Y]_\nu,\ [Y]_0=\frac{1}{pL_{cm}}\begin{bmatrix}1&1\\1&1\end{bmatrix},$$

$$[Y]_\nu=\frac{2p}{p^2+\omega_\nu^2}\left[k_{mn}^{(\nu)}\right],\ \nu=1,2, \quad (25)$$

Where L_{st} is the static inductance of the line; $\left[k_{mn}^{(\nu)}\right]$ - matrix of residues of the elements of the matrix of conductivities in the poles $p_\nu = j\omega_\nu,\ \nu = 1,2,3,...,\ m = 1,2;\ n = 1,2$.

$$\left[k_{mn}^{(\nu)}\right] = \begin{bmatrix} resZ_{11} & resZ_{12} \\ resZ_{12} & resZ_{22} \end{bmatrix} \tag{26}$$

From (25), (26) it follows that in the region of the anti-resonant frequency ω_ν , that is, in the region of the pole $p_\nu = j\omega_\nu$, the approximate equality takes place:

$$[Y] \approx [Y]_\nu = \begin{bmatrix} \dfrac{2k_{11}^{(\nu)}p}{p^2+\omega_\nu^2} & \dfrac{2k_{12}^{(\nu)}p}{p^2+\omega_\nu^2} \\ \dfrac{2k_{12}^{(\nu)}p}{p^2+\omega_\nu^2} & \dfrac{2k_{22}^{(\nu)}p}{p^2+\omega_\nu^2} \end{bmatrix} \tag{27}$$

In this case, as in the case of the impedance matrix, the line is a compact four-pole.

$$k_{11}^{(\nu)}k_{22}^{(\nu)} - \left(k_{12}^{(\nu)}\right)^2 = 0. \tag{28}$$

Consider the conductivity matrix of the circuit in Figure 3.

$$[Y] = \begin{bmatrix} \dfrac{\frac{1}{L_\nu}p}{p^2+\omega_\nu^2} & \dfrac{-\frac{1}{nL_\nu}p}{p^2+\omega_\nu^2} \\ \dfrac{-\frac{1}{nL_\nu}p}{p^2+\omega_\nu^2} & \dfrac{\frac{1}{n^2L_\nu}p}{p^2+\omega_\nu^2} \end{bmatrix}. \tag{29}$$

To determine the elements of the equivalent circuit, we equate (29) and (27). As a result, we get:

$$L_\nu = \frac{1}{2k_{11}^{(\nu)}},\ C_\nu = \frac{2k_{11}^{(\nu)}}{\omega_\nu^2},\ n = -\frac{k_{11}^{(\nu)}}{k_{12}^{(\nu)}} = -\frac{k_{12}^{(\nu)}}{k_{22}^{(\nu)}}. \tag{30}$$

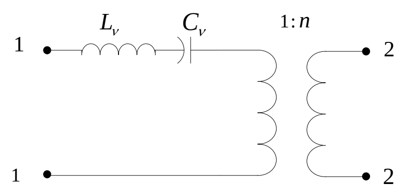

Figure 3. Equivalent circuit of a non-homogeneous line in the region of anti-resonant frequencies

The parameters of the second equivalent circuit in the region of antiresonant frequencies are determined similarly. For the circuit in Figure 4, the admittance matrix is:

$$[Y] = \begin{bmatrix} \dfrac{\frac{m^2}{L_\nu}p}{p^2+\omega_\nu^2} & \dfrac{-\frac{m}{L_\nu}p}{p^2+\omega_\nu^2} \\ \dfrac{-\frac{m}{L_\nu}p}{p^2+\omega_\nu^2} & \dfrac{\frac{1}{L_\nu}p}{p^2+\omega_\nu^2} \end{bmatrix}. \tag{31}$$

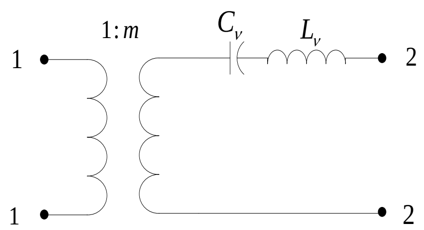

Figure 4. The second equivalent circuit of a non-homogeneous line in the region of antiresonance frequencies

Equating (27) and (31), we find the equivalence conditions:

$$L_v = \frac{1}{2k_{22}^{(v)}},\ C_v = \frac{2k_{22}^{(v)}}{\omega_v^2},\ m = -\frac{k_{11}^{(v)}}{k_{12}^{(v)}} = -\frac{k_{12}^{(v)}}{k_{22}^{(v)}}. \qquad (32)$$

2.4. Filters With Parallel Resonators

Calculation formulas for the scheme of Figure 5 [10]:

$$b_j = \frac{\omega_0}{2}\frac{dB_j(\omega)}{d\omega}.\ \omega = \omega_0,\ J_{01} = \sqrt{\frac{G_A b_1 w}{g_0 g_1 \omega_1^{'}}},$$
$$J_{j,j+1} = \frac{w}{\omega_1^{'}}\sqrt{\frac{b_j b_{j+1}}{g_j g_{j+1}}},\ j = 1,....n-1; \qquad (33)$$
$$J_{n,n+1} = \sqrt{\frac{G_B b_n w}{g_n g_{n+1} \omega_1^{'}}},\ w = \frac{\omega_2 - \omega_1}{\omega_0},\ \omega_0 = \sqrt{\omega_1 \omega_2}.$$

Where $g_0, g_1, ..., g_{n+1}$ - LPF prototype parameters; bandwidth LPF prototype; $B_k(\omega), (k = 1, 2, ..., n)$ - conductivity of the parallel oscillatory circuit.

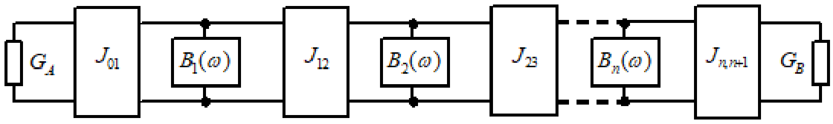

Figure 5. Generalized BPF circuit with admittance inverters [20]

Let's replace the parallel circuits with irregular transmission lines (Figure 6).

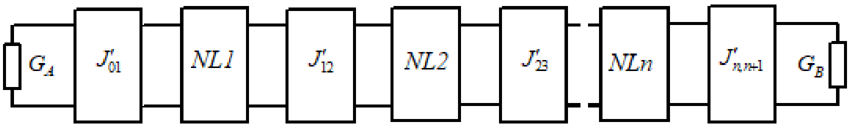

Figure 6. Generalized BPF circuit for NL with admittance inverters

Since J-inverters (conductivity inverters) provide high- impedance loads NL, then in the region of resonant frequency the link "NL - inverter" has an equivalent circuit in Figure7.

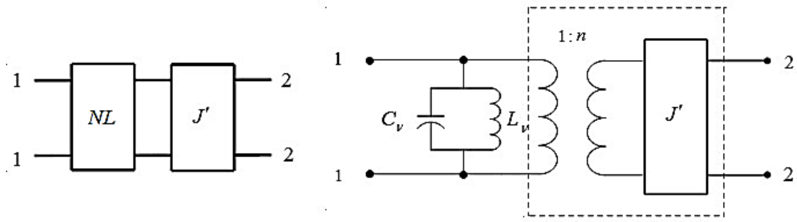

Figure 7. Equivalent circuit of the "NL - inverter" link in the resonant frequency region

Let's find the chain matrix of the connection "ideal transformer - inverter" (Figure 7):

$$A = \begin{bmatrix} \frac{1}{n} & 0 \\ 0 & n \end{bmatrix} \begin{bmatrix} 0 & \pm\frac{j}{J'} \\ \pm jJ' & 0 \end{bmatrix} = \begin{bmatrix} 0 & \pm\frac{j}{nJ'} \\ \pm jnJ' & 0 \end{bmatrix}. \qquad (34)$$

Thus, the four-pole, circled by a dotted line in Figure 7, is an inverter of conductivities with an inversion coefficient. Therefore, in order for the circuits in Figure 5 and 6 to be equivalent, the condition must be met for all links of the NL - inverter. As a result, we obtain the equivalence condition for both schemes:

$$J'_{01} = J_{01},\ J'_{12} = \frac{J_{12}}{n},\ J'_{23} = \frac{J_{23}}{n}, ..., J'_{n,n+1} = \frac{J_{n,n+1}}{n}. \qquad (35)$$

Therefore, formulas (33) should be used when calculating the BPF on the NL. But the inversion coefficients must be determined based on conditions (35).

If we use the second equivalent NL circuit (Figure 2), then we should consider the “inverter - NL” links in the resonant frequency region. Chain matrix connection "inverter - ideal transformer":

$$A=\begin{bmatrix}0 & \pm\frac{j}{J'}\\ \pm jJ' & 0\end{bmatrix}\begin{bmatrix}\frac{1}{m} & 0\\ 0 & m\end{bmatrix}=\begin{bmatrix}0 & \pm\frac{jm}{J'}\\ \pm j\frac{1}{m}J' & 0\end{bmatrix}. \quad (36)$$

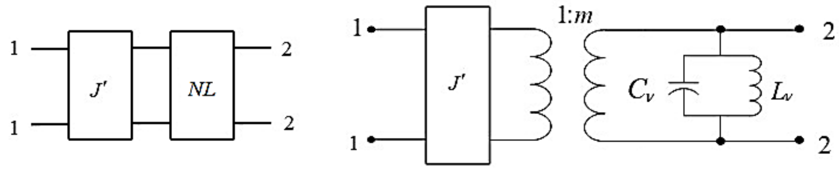

Figure 8. Equivalent circuit of the "inverter - NL" link in the resonant frequency region

Expression (20) corresponds to the conductivity inverter with the inversion coefficient $\frac{J'}{m}$. Therefore, for the equivalence of the circuits in Figure 5 and Figure 6, it is necessary to fulfil the condition $\frac{J'}{m}=J$, i.e.

$$J'_{01}=mJ_{01},\ J'_{12}=mJ_{12},\ J'_{23}=mJ_{023},\ ...,J'_{n,n+1}=mJ_{n,n+1}. \quad (37)$$

3. RESULTS AND DISCUSSION

This section presents the results of the mathematical synthesis of series resonator filters. A synthesized scheme of three stub prototype BPF is presented. A study of the amplitude-frequency characteristic of the BPF prototype was carried out.

3.1. Series Resonator Filters

Calculation formulas for the scheme of Figure 9 [20]:

$$x_j=\frac{\omega_0}{2}\frac{dX_j(\omega)}{d\omega},\ \omega=\omega_0,\ K_{01}=\sqrt{\frac{R_A x_1 w}{g_0 g_1 \omega_1^{'}}},$$
$$K_{j,j+1}=\frac{w}{\omega_1^{'}}\sqrt{\frac{x_j x_{j+1}}{g_j g_{j+1}}},\ j=1,....n-1; \quad (38)$$
$$K_{n,n+1}=\sqrt{\frac{R_B x_n w}{g_n g_{n+1}\omega_1^{'}}},\ w=\frac{\omega_2-\omega_1}{\omega_0},\ \omega_0=\sqrt{\omega_1\omega_2}.$$

Where x_j is the parameter of the steepness of the reactance; $X_k(\omega), (k=1,2,...,n)$ - reactive impedance of series circuits.

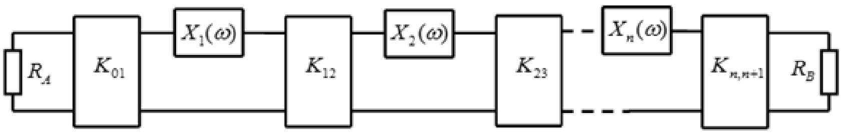

Figure 9. Generalized BPF circuit with impedance inverters

In the scheme Figure 10, we replace the reactivity by NL.

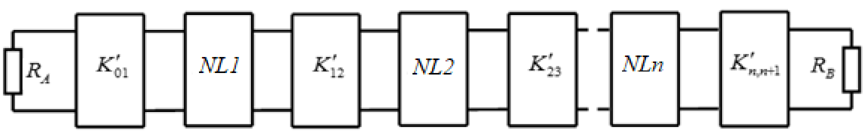

Figure 10. Generalized scheme of BPF on NL with impedance inverters

From here we find the equivalent circuit of the NL-inverter link.

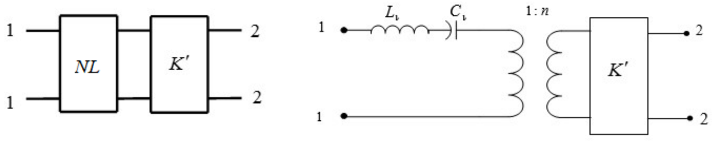

Figure 11. Link "NL- impedance inverter" and its equivalent circuit in the region of antiresonant frequency

We find the A-matrix of the transformer-inverter connection (Figure 11):

$$A=\begin{bmatrix}\frac{1}{n} & 0\\ 0 & n\end{bmatrix}\begin{bmatrix}0 & \pm jK'\\ \pm\frac{j}{K'} & 0\end{bmatrix}=\begin{bmatrix}0 & \pm\frac{jK'}{n}\\ \pm\frac{jn}{K'} & 0\end{bmatrix}. \quad (39)$$

The equivalence condition for the circuits in Figure 9 and Figure 10 is:

$$K'_{01}=K_{01},\ K'_{12}=K_{12}n,\ K'_{23}=K_{23}n,...,K'_{n,n+1}=K_{n,n+1}n. \quad (40)$$

Based on the second scheme in Fig. 4, the equivalence condition can be written as:

$$K'_{01}=\frac{K_{01}}{m},\ K'_{12}=\frac{K_{12}}{m},K'_{23}=\frac{K_{23}}{m},...,K'_{n,n+1}=\frac{K_{n,n+1}}{m}. \quad (41)$$

Where *e(x)* is error, x_{ref} is reference position and *x* is actual position.

3.2. Research BPF Prototypes

According to the formulas obtained, BPF prototypes were synthesized with two parallel plumes based on a closed homogeneous line and one plume based on three NLs with wave impedances $\frac{W_{0i}}{ch^2 a_i\tau}$, $(i=1,2,3)$ (Figure 12, Figure 13) with the initial data:

- relative bandwidth ω=0.05; 0.15; 0.3;
- attenuation in the passband $L_r=2dB$;
- load conductivity $Y_A=Y_B=1\,S$;
- the center frequency of the first parasitic passband is 7 times the center frequency of the passband.

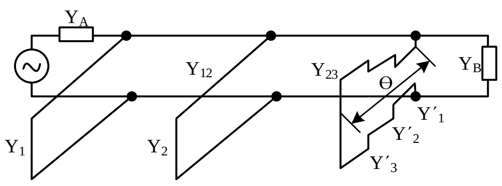

Figure 12. Scheme of three stub prototype BPF: wave conductivities Y'_1,Y'_2,Y'_3 of a three-stage NL change according to the law $(W_{0i}/ch^2 a_i\tau)^{-1}$, $(i=1,2,3)$

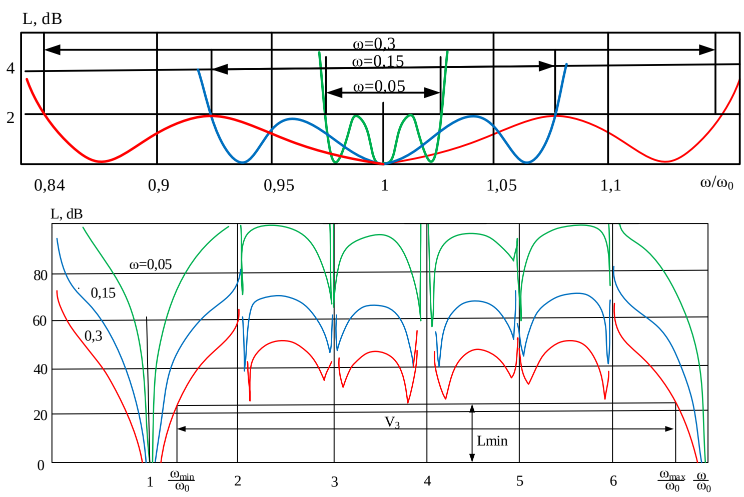

Figure 13. Amplitude-frequency characteristic of the BPF prototype; ω_0 - center frequency of the passband, V_s - width of the blocking area, L_{min} - minimum attenuation in the blocking area

As the first two resonators, we took homogeneous closed segments of transmission lines with delay time $\pi/2\omega_0$ and wave conductivities:

$Y_1 = 66,5S(\omega = 0,05);\quad 20,5S(\omega = 0,15);\quad 9S(\omega = 0,3);$

$Y_2 = 133S(\omega = 0,05);\quad 41S(\omega = 0,15);\quad 18S(\omega = 0,3).$

The third resonator is formed by three NLs with the same delay times, connected in cascade (Figure 12), with a total electrical length θ=1.178 radians and wave conductivities

$$Y_k^1 = \left(\frac{W_0}{ch^2 a\tau}\right)^{-1}, k = 1,2,3. \quad (42)$$

In this case, different values of k correspond to different values of W_0.

At $\omega = 0,05$ the delay time of each stage for different relative bandwidths are the same: $t' = 0,4/\omega_0,\ 0 \le \tau \le t'$. Step impedances:

W_0 are (42): $W_{01} = 2Ohm, W_{02} = 4,8Ohm,\ W_{03} = 9,2Ohm.$

For $\omega = 0,15$ $W_{01} = 2Ohm, W_{02} = 4,8Ohm,\ W_{03} = 9,2Ohm.$

For $\omega = 0,3$ $W_{01} = 5,5Ohm, W_{02} = 10,8Ohm,\ W_{03} = 16,2Ohm.$

The resonators are interconnected by quarter-wave transformers (inverters) on homogeneous transmission lines with wave impedances W=14.3 *Ohm*.

Further research is related to the development of broadband matching devices based on heterogeneous lines for matching complex loads of high-speed information transmission systems.

4. CONCLUSION

From the analysis of the obtained results it follows:

1. When synthesizing BPF based on NL, one can use the Cohn method and other methods of filter synthesis. In this case, when using resonators made on the NL, one should take into account the presence of an additional transformer, which introduces a correction in determining the parameters of the inverters.

2. The use of NLs as resonators makes it possible, by choosing the wave impedance, to increase the stopband of the BPF in comparison with the BPF on resonators based on uniform lines. In particular, if only homogeneous lines are used as resonators, then the first two spurious bandwidths will appear at $\omega/\omega_0 = 3, 5$.

3. As the bandwidth increases, the attenuation minimum in the blocking region decreases.

4. The frequency response in the area of the barrier is strongly jagged. The attenuation maximum occurs at the serial resonance frequencies of the parallel loops. The attenuation minima are located between these frequencies. Therefore, to increase the attenuation in the blocking region, it is necessary to use resonators with a rarefied frequency spectrum of parallel and series resonance.

REFERENCES

[1] A. S. Alam, Y. -F. Hu, P. Pillai, K. Xu and J. Baddoo, "Optimal Datalink Selection for Future Aeronautical Telecommunication Networks," *IEEE Transactions on Aerospace and Electronic Systems*, vol. 53, no. 5, pp. 2502-2515, Oct. 2017, https://doi.org/10.1109/TAES.2017.2701918.

[2] H. N. Uzo, U. Oparaku Ogbonna, and V. C. Chijindu, "Design of FIR digital filters using Semi-ellipse window," *Indonesian Journal of Electrical Engineering and Informatics (IJEEI)*, vol. 9, no. 3, pp. 647-661, Sept. 2021, https://doi.org/10.52549/ijeei.v9i3.2481.

[3] L. Mohammed, T. Islam, and Z. Lahbib, "Performance Analysis of Low noise amplifier using Combline Bandpass Filter for X Band Applications," *Indonesian Journal of Electrical Engineering and Informatics (IJEEI)*, vol. 7, no.3, pp. 535-542, Sep 2019, https://doi.org/10.11591/ijeei.v7i3.1012.

[4] M. Omar, N. A. M. Zin, Z. I. A. Latiff, and N. A. Ismail, "Review on design of on chip band pass filter for radio frequency applications," *2016 7th IEEE Control and System Graduate Research Colloquium (ICSGRC)*, Shah Alam, Malaysia, 2016, pp. 148-152, https://doi.org/10.1109/ICSGRC.2016.7813318.

[5] T. George, and B. Lethakumary, "High frequency rejection using L shaped defected microstrip structure in ultra wideband bandpass filter," *Materials Today: Proceedings*, vol. 25, patr 2, pp. 265-268, Feb. 2020, https://doi.org/10.1016/j.matpr.2020.01.363.

[6] K. -R. Xiang, and F. -C. Chen, "Compact Microstrip Bandpass Filter With Multispurious Suppression Using Quarter-Wavelength and Half-Wavelength Uniform Impedance Resonators," *IEEE Access*, vol. 6, pp. 20364-20370, 2018, https://doi.org/10.1109/ACCESS.2018.2822262.

[7] S. Fu, C. Lian, Z. Xu, and Z. Wang, "Design of highly selective balanced bandpass filter with wide differential-mode stopband and high common-mode suppression," *AEU - International Journal of Electronics and Communications*, vol. 178, pp. 155262, May 2024, https://doi.org/10.1016/j.aeue.2024.155262.

[8] D.M. Pozar, *Microwave engineering*. 4th ed. New York: John Wiley & Sons, 2012.

[9] R.J. Cameron, C.M. Kudsia, and R.R. Mansour, *Microwave Filters for Communication Systems: Fundamentals, Design, and Applications*. New York: John Wiley &Sons, 2018, https://doi.org/10.1002/9781119292371.
[10] S. Gruszczynski, K. Staszek, and K. Wincza, "Parallel-coupled bandpass filters with directly coupled input and output resonators," *AEU - International Journal of Electronics and Communications*, vol. 172, pp. 154974, Dec. 2023, https://doi.org/10.1016/j.aeue.2023.154974.
[11] Y. Zhang, F. Seyfert, S. Amari, M. Olivi, and K. -L. Wu, "General Synthesis Method for Dispersively Coupled Resonator Filters With Cascaded Topologies," *IEEE Transactions on Microwave Theory and Techniques*, vol. 69, no. 2, pp. 1378-1393, Feb. 2021, https://doi.org/10.1109/TMTT.2020.3041223.
[12] G. Lee, J. Lee, Bo.Lee, and J. Lee, "Rigorous design method for distributed-element bandpass filter with reflectionless response at two ports," *Electronics Letters*, vol. 57, iss. 13, pp. 514-516, May 2021. https://doi.org/10.1049/ell2.12182.
[13] V. Kozlovskyi, *et al.*, "Low-Frequency Schemes of Substitution of Segments Inhomogeneous Transmission Lines," *2019 IEEE 3rd International Conference on Advanced Information and Communications Technologies (AICT)*, Lviv, Ukraine, 2019, pp. 80-83, https://doi.org/10.1109/AIACT.2019.8847844.
[14] A. Ametani, K. Yamamoto, and N.Triruttanapiruk, "Non-uniform lines – review of the theory and measured / simulation examples," *Electric Power Systems Research*, vol. 188, pp. 106514, Nov. 2020, https://doi.org/10.1016/j.epsr.2020.106514.
[15] J. Valencia, V. E. Boria, M. Guglielmi, and S. Cogollos, "Compact Wideband Hybrid Filters in Rectangular Waveguide With Enhanced Out-of-Band Response," *IEEE Transactions on Microwave Theory and Techniques*, vol. 68, no. 1, pp. 87-101, Jan. 2020, https://doi.org/10.1109/TMTT.2019.2947911.
[16] J. F. Valencia Sullca, M. Guglielmi, S. Cogollos, and V. E. Boria, "Hybrid Wideband Staircase Filters in Rectangular Waveguide With Enhanced Out-of-Band Response," *IEEE Transactions on Microwave Theory and Techniques*, vol. 69, no. 8, pp. 3783-3796, Aug. 2021, https://doi.org/10.1109/TMTT.2021.3076061.
[17] O. Shynkaruk, J. Boiko and O. Eromenko, "Measurements of the energy gain in the modified circuit signal processing unit," *2016 IEEE 13th International Conference on Modern Problems of Radio Engineering, Telecommunications and Computer Science (TCSET)*, Lviv, Ukraine, 2016, pp. 582-584, https://doi.org/10.1109/TCSET.2016.7452121.
[18] C. Guo, X. Shang, M. J. Lancaster, and J. Xu, "A 3-D Printed Lightweight X-Band Waveguide Filter Based on Spherical Resonators," *IEEE Microwave and Wireless Components Letters*, vol. 25, no. 7, pp. 442-444, July 2015, https://doi.org/10.1109/LMWC.2015.2427653.
[19] E. López-Oliver *et al.*, "3-D Printed Bandpass Filter Using Conical Posts Interlaced Vertically," *2020 IEEE/MTT-S International Microwave Symposium (IMS)*, Los Angeles, CA, USA, 2020, pp. 580-582, https://doi.org/10.1109/IMS30576.2020.9223965.
[20] V. V. Kozlovskyi, V. V. Kozlovskyi, R. V. Khrashchevskyi, and V. V. Klobukov, "Determination of the transmission line resistance matrix with deviations of design parameters from nominal", *Radio Electronics, Computer Science, Control*, no. 2, p. 7, Jun. 2022, https://doi.org/10.15588/1607-3274-2022-2-1.
[21] S. Cogollos, R. J. Cameron, M. Guglielmi, J. C. Melgarejo, and V. E. Boria, "Inductive Cascaded Quadruplet With Diagonal Cross-Coupling in Rectangular Waveguide," *IEEE Access*, vol. 10, pp. 45241-45255, 2022, https://doi.org/10.1109/ACCESS.2022.3169774.
[22] G.T. Bharathy, S.Bhavanisankari, T. Tamilselvi, and G. Bhargavi,"Analysis and Design of RF Filters with Lumped and Distributed Elements," *International Journal of Recent Technology and Engineering (IJRTE)*, vol. 8, iss. 2S5, pp. 38-42, 2020, https://doi.org/10.35940/ijrte.B1009.0782S519.
[23] Z. Yi et al., "Dual-frequency switchable bandpass filter in the terahertz range based on enhanced trapped-mode resonances," *Chemical Physics Letters*, vol. 826, pp. 140637, Sep. 2023, https://doi.org/10.1016/j.cplett.2023.140637.

BIOGRAPHY OF AUTHORS

Valeriy Kozlovskiy graduated from the Kyiv Higher Military Aviation Engineering School (Ukraine) in 1992, with the qualification of a Radio Engineer. In 1994, he received the Ph.D. in Armament and military equipment at the Kyiv Air Force Institute. In 2013, he received the D.Sc. at the State University of Information and Communication Technologies (Kyiv). In 2014, he received the academic title of professor. Since 2014, he held the position of head of the Information Protection Department of the Educational and Scientific Institute of Information and Diagnostic Systems of the National Aviation University. Since 2018 he held the position of the first vice-rector of the National Aviation University. From 2020 currently he is the head of the Department of Information Protection, National Aviation University (Kyiv, Ukraine). His research interests are: intelligent decision-making support systems, information protection management, end-to-end control and optimization in information and calculating networks.
You can contact him by e-mail: vvkzeos@gmail.com

Valerii Kozlovskiy graduated from Kyiv Higher Aviation Engineering Military School (Ukraine) in 1970. Doctor of Technical Sciences (1985), professor (1987). 2002 – 2005 he held the Head position of the Department of Special Problems of Science and Technology of the Higher Attestation Commission of Ukraine. From 2006 - Head of the Special Department No. 4 of the Institute of Special Communication and Information Protection, National Technical University of Ukraine "Kyiv Polytechnic Institute". Currently, Full Professor of the Institute of Special Communication and Information Protection, National Technical University of Ukraine "Igor Sikorsky Kyiv Polytechnic Institute" (Kyiv, Ukraine). Research interests: radio electronics, ultra-high frequencies techniques, nonregular distributed circles.
You can contact him by e-mail: valerey@ukr.net

Juliy Boiko received his Specialist Degree and a Radio Design Engineer qualification from the Technological University of "Podillya" (Ukraine) in 1998. In 2002 he received a Candidate of Science degree (PhD) at the Institute of Electrodynamics of the National Academy of Sciences of Ukraine in the field of device design and development of methods for measuring electrical and magnetic quantities. In 2015, he received a Doctor of Science degree (D.Sc. in Engineering) at the State University of Telecommunications (Kyiv, Ukraine) in the field of signal reception, synchronization, signal processing in telecommunication systems. Currently, Full Professor of the Department of Telecommunications, Media and Intelligent Technologies, Khmelnytskyi National University (Khmelnytskyi, Ukraine). Research includes issues related to the development of devices for the automation of devices and systems, the theory of coding, synchronization systems, diagnostics and signal processing. You can contact him by e-mail: boiko_julius@ukr.net.

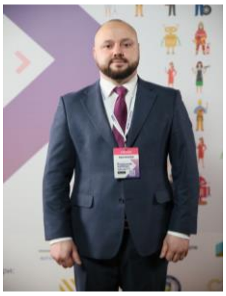

Yuriy Balanyuk received a Master's Degree in the field of electronics and telecommunications and a Radio Design Engineer qualification from the National University "Lviv Polytechnic" (Ukraine) in 2007. In 2017 he received a Candidate of Science degree (PhD) in radio engineering and television systems. Since 2019, he has been the head of the National Qualifications Agency. Currently, Associate Professor of the Department of Information Protection System, National Aviation University (Kyiv, Ukraine). Research includes issues related to cybersecurity outlines, distributed circuits synthesis. You can contact him by e-mail: y.balanyuk@nqa.gov.ua

Natalia Yakymchuk received a Master's Degree in automated control of technological processes at the Lutsk State Technical University (Ukraine) in 2005. In 2023 she received a Candidate of Science degree (PhD) at the National Aviation University (Kyiv, Ukraine) in the field of telecommunication systems and networks. Currently, assistant of the Department of Electronics and Telecommunications of the Lutsk National Technical University (Lutsk, Ukraine). Research includes issues related to diagnostics and control of the telecommunication networks state, congestion management. You can contact she by e-mail: n.yakymchuk@lntu.edu.ua